Soldagem & Inspeção

ISSN 1980-6973 (Online) | ISSN 0104-9224 (Print)
INVITED PAPERS

Influence of Forging Pressure on Microstructural and Mechanical Properties Development in Linear Friction Welded Al-Cu Dissimilar Joint

Nan Zhou[1,2,3], Chunlei Gan[1,3], Dongfu Song[1,3], Wenjun Qi[1], Moataz M. Attallah[2]

[1] Guangdong Institute of Materials and Processing, Guangzhou, China.
[2] The University of Birmingham, School of Metallurgy and Materials, Edgbaston, United Kingdom.
[3] Guangdong Province Key Laboratory for Technology & Application of Metal Toughening, Guangzhou, China.

How to cite: Zhou N, Gan C, Song D, Qi W, Attallah MM. Influence of forging pressure on microstructural and mechanical properties development in linear friction welded Al-Cu dissimilar joint. Soldagem & Inspeção. 2019;24:e2401. https://doi.org/10.1590/0104-9224/SI2304.08

Abstract: Dissimilar AA5083 and C101 pure copper linear friction welds were prepared using different forging pressures (60 MPa, 80 MPa, and 110 MPa) to investigate the influence of the forging pressure on the microstructural and mechanical properties development using optical microscopy (OM), scanning electron microscopy (SEM), hardness measurements, and tensile testing. The in-situ generated intermetallic particles in the vicinity of the weld line were characterised using electron probe micro-analyser (EPMA), to rationalise their impact on the mechanical properties. The results showed that the process led to the formation of various intermetallic phases as well as the entrainment of base material fragments in the vicinity of the weld interface. In general, high forging pressure corresponding to high welding heat input resulted in the formation of a layered intermetallic phase (identified as Al_2CuMg), which was the most detrimental to the mechanical properties, compared with a scattered distribution of fragmented Cu and intermetallic particles across the joint interface.

Key-words: Linear Friction Welding (LFW); Forging pressure; Intermetallic compound; Mechanical properties.

1. Introduction

Linear friction welding (LFW) is a rapidly growing solid state joining process that has been successfully applied in various components, notably for producing integrated bladed disks assemblies (blisks) in aeroengines [1,2]. During LFW, the workpieces are firstly brought into contact, followed by oscillating one workpiece, while maintaining the other stationary. Frictional heating, combined with plastic deformation, results in a rapid temperature increase, creating a sideward extrusion of the softened material, thus achieving consolidation within seconds, and then the forging pressure is performed in the final stages to enhance the consolidation. Due to its solid-state nature, the process is viable for the production of high strength dissimilar joints [3-8], especially Al-Cu joints that are used in the power transmission applications due to the excellent electrical conductivities of Al and Cu. For Al and its alloys, the conductivity-to-density ratio is twice that of copper, making a strong industrial case for dissimilar Al-Cu joints for component weight reduction, in addition to the cost savings due to the lower cost of Al-alloys compared with Cu.

The quality of the Al-Cu joints depends on the weld microstructure formed, especially the presence of intermetallic phases, due to their detrimental influence on the mechanical properties [9,10]. Because of the differences in thermal expansion coefficients and hardness between the intermetallic phases and the base metal matrices, cracks may form at the interface in the weld metal when stressed, significantly reducing its mechanical properties [11]. According to the binary Al-Cu phase diagram [12], five types of thermodynamically stable intermetallic phases may exist, which are: $CuAl_2$ (θ), CuAl (η), Cu_4Al_3 (ζ), Cu_3Al_2 (δ), and Cu_9Al_4 (γ). Due to the mismatch in lattice constants and thermal expansion coefficients between the intermetallic phases and the base metal matrices, large internal stresses are produced at the joint line, decreasing the bonding strength of the interface [13]. Furthermore, intermetallic phases are known to have a high hardness and electrical resistivity [8,10], which are likely to increase the brittleness of the joint and reduce the conductivity of the joint, respectively. Wanjara et al. [14] investigated dissimilar joints of AA6063 to pure Cu. $CuAl_2$ and Cu_2Al were found using EDX along the joint interface, showing a layered structure. It is possible to optimise LFW parameters to avoid the formation of large layers of intermetallic phases, as in the work of Bhamji et al. [7]. In their work, LFW of AA1050 to copper (C101) resulted only in copper particles in Al parent metal side close to the joint interface.

Received: 15 Feb., 2019. Accepted: 15 Feb., 2019.
E-mails: nxz496@student.bham.ac.uk (NZ), ganchunlei@163.com (CG), 375462908@qq.com (DS), qiwenjun987@sohu.com (WQ), m.m.attallah@bham.ac.uk (MMA)

As the review of the literature has shown, the generation of Al-Cu intermetallic compounds is detrimental to the joint mechanical properties. As a result, effective control of the formation and growth of intermetallic compounds is essential to achieve an acceptable performance. This study focuses on the influence of LFW parameters, especially the forging pressure on the microstructure and mechanical properties of dissimilar AA5083-H112 aluminium alloy and C101 Cu joints. The study also assesses the influence of the forging pressure on the type, size, and distribution of the Al-Cu intermetallic compounds, so as to optimise the welding parameters and reduce the generation of the Al-Cu intermetallic compounds.

2. Material and Experimental Methods

The base materials used for LFW in this study were AA5083 (in H112 condition) alloy and C101 Cu copper rolled plates. The plates were cut to the dimension of *(x,y,z)* 55×30×15 mm with the weld interface of located on the *yz*-plane and *y*-being the reciprocation direction. The chemical composition of the materials is shown in Table 1.

Table 1. Chemical composition of the parent materials (wt. %).

Material	Si	Fe	Cu	Mn	Mg	Zn	Cr	Ti	Others	Al
AA5083	0.4	0.1	0.1	0.6	4.0	0.2	0.15	0.1	≤0.15	Bal.
C101-Cu	-	-	≥99.9	-	-	-	-	-	<0.1	-

The welds were produced using a custom-built electromechanical LFW machine based at Northwestern Polytechnical University in Xi'an, China. Prior to welding, the surfaces of the coupons were ground and wiped using acetone to get rid of any surface oxide and oil contamination. In the welding process, three levels of forging pressures (60, 80, 110 MPa) were performed after the oscillation, while the oscillation frequency and amplitude were kept constant as 35 Hz and 2.5 mm, respectively. The Cu weld side was reciprocated while the Al side was held stationary (see Figure 1).

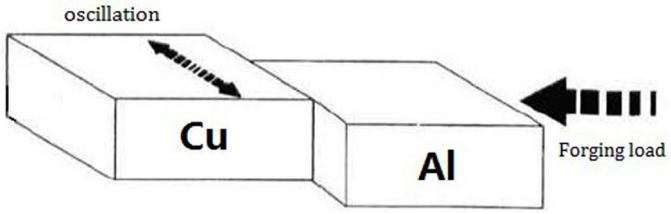

Figure 1. Schematic diagram of LFW process.

All the welds were left to cool after welding.

Metallographic specimens were extracted normal to the weld interface along the *xz*-plane and *yz*-plane, ground, and polished to produce a mirror-like finish. Keller's reagent (3 mL HNO_3, 6 mL HCl, 6 mL HF, and 150 mL distilled H_2O) was used to etch the Al samples and a solution of 5g $FeCl_3$, 10 mL HCl, 100 mL distilled H_2O was used to etch the Cu samples to reveal the grain structure. The microstructures were examined using a LEICA-DMI3000M optical microscope (OM). The intermetallic particles at Al-Cu interface were examined under a FEI Nova Nano 430 scanning electron microscope (SEM) and a JEOL JXA-8100 electron-probe microanalyser (EPMA) to identify the types of the intermetallic phases.

Room temperature tensile test samples were tested in accordance with BS EN 10002-1:2001 for LFW joints, with the samples loaded normal to the weld interface to test the bond strength. The tests were carried out on the DNS200 universal tensile testing machine, with a crosshead speed of 2 mm/min, with 3 replicates per condition. The Vickers hardness was measured at mid-thickness of the sheets along the normal direction using a microhardness analyser at a load of 5 kg force and a dwell period of 10 s, with the indentations performed at 1 mm spacing in the *x*-direction.

3. Results and Discussion

3.1. Microstructure evolution

Figure 2 shows the parent materials microstructures and the microstructure of the defect free LFW joint. Elongated grains oriented along the rolling direction can be observed in the parent Al-alloy (Figure 2a). Annealed twins and coarse grains with the average grain size of 105µm were observed in the parent pure Cu (Figure 2b). Figure 2c shows the interface

microstructure of the LFW joint. Fine recrystallised equiaxed grains (down to ~1 µm) were observed close to the interface on the Al-side. On the Cu side, a clear demarcation was observed between the recrystallised Cu grain region close to the weld interface and the deformed Cu grains further away from the weld region, which are elongated along the oscillation direction.

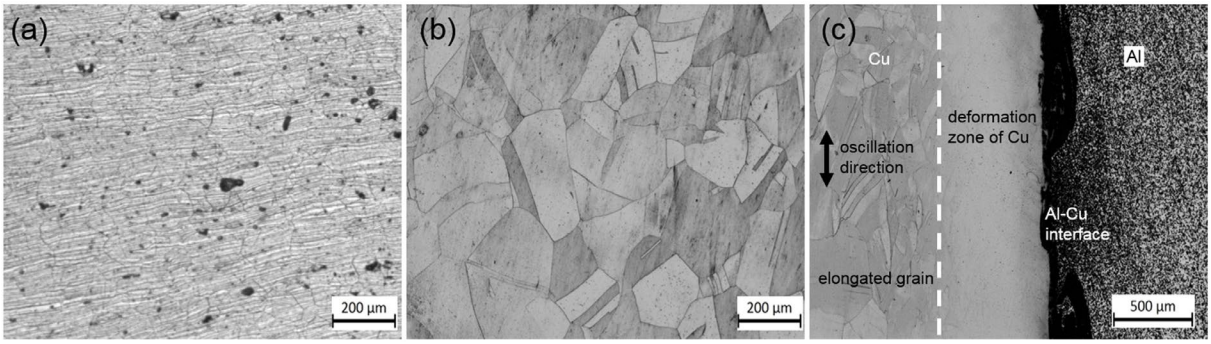

Figure 2. Microstructures of the Al-Cu LFW joint. (a) Al base metal; (b) Cu base metal; (c) Al-Cu interface showing the weld regions.

Figure 3 shows the backscattered SEM micrographs for the transition region across the weld interface. The micrographs show an intimate contact between the two materials with no obvious structural defect (e.g. cracks of all types). However, intermetallic particles are present along the joint interface in all the welds, appearing as fine discontinuous particles along the Al side and layered structures along the Cu side. The fine particles were observed in all the welds, with more particles being present with the decrease in the forging pressure. Furthermore, the layered intermetallic phases formed on the edge of the Cu side. It is important to note that the layered intermetallic phase was more prominent in the higher forging pressure samples (Figure 3a, b, d and e), whereas in the low forging pressure samples, the layered intermetallic phase could hardly be detected along the interface. Instead, fragmented Cu-rich particles were seen at the joint interface. In general, Cu fragments were entrained in the Al side in most welds (Figure 3b, c, e, and f). At the forging pressure of 110 MPa, Cu fragments could hardly be found in the in the Al side. With the decrease of the forging pressure, the Al-Cu mechanical mixing and fragmentation process was severer, and more copper particle fragments were entrained due to the insufficient thermal fields to promote diffusion between the Al and Cu sides of the joints.

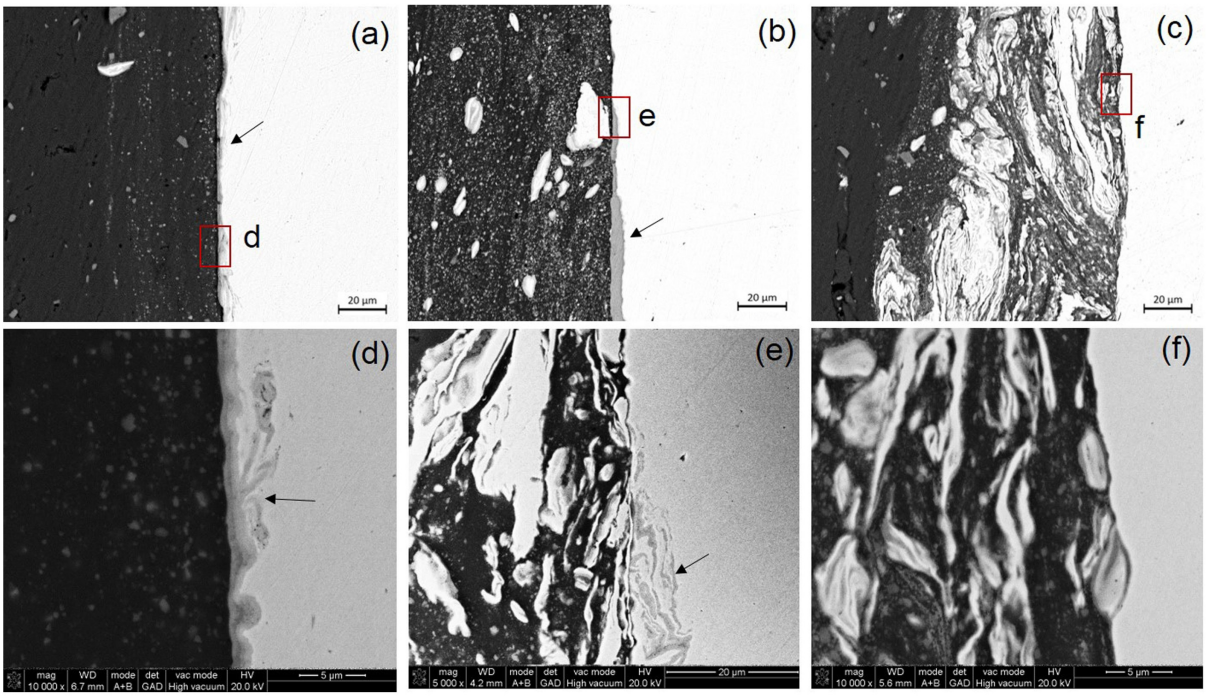

Figure 3. SEM backscattered electron micrographs of the joint, showing the Al side (left) and Cu side (right), welded using different forging pressures. (a); (d) 110 MPa; (b); (e) 80 MPa; (c); (f) 60 MPa.

Figure 4 shows the EDX analyses of the particles (a) and layered (b) intermetallic phase at the joint interface. It was found that the fine particles (marked "a" in Figure 4a) in the Al matrix had the main composition of Al, Mg and Cu, with the Al-Cu-Mg ratio of 78.8:10.7:10.4. Besides, apart from the Al matrix, intermetallic particles are also present in the Cu-rich fragments which were entrained in the Al-side. In Figure 4a, two types of intermetallics were detected in the Cu-rich fragments, which have fragmented and multi-layered structures (marked "b" and "c"), respectively. EDX results showed that the Al-Cu ratio of the intermetallic particle was 66.5:33.5 (in atomic%), which was close to $CuAl_2$ (θ phase), and the Al-Cu ratio of the layered intermetallic phase was 27.8:72.2, close to Cu_9Al_4, (γ phase). Moreover, a layered intermetallic phase can be observed between Al and Cu matrix. Figure 4b shows the EDX line scan results, which is showing that the layered intermetallic phase is (Al, Cu)-rich, in addition to Mg. Due to the Mg content in the base Al-alloy, it is possible to suggest that the layered intermetallic phase could be an Al-Mg-Cu ternary phase.

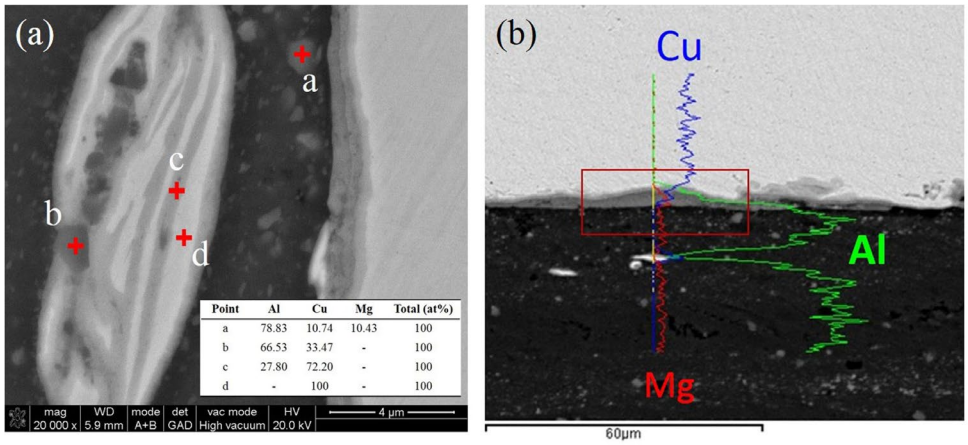

Figure 4. EDX analyses of the particle (a) and layered (b) intermetallic phase at the joint interface.

3.2. Hardness distribution

A hardness trace across the joint line showed that the hardness increased close to the weld line on both weld sides (see Figure 5). A hardness peak was present at the vicinity of the joint interface, with no obvious drop in hardness due to the heat-affected zone (HAZ). The peak hardness was the highest at the forging pressure of 80 MPa (~137 HV), whereas the 110 MPa and 60 MPa showed hardness peaks of 87 HV and 107 HV, respectively, significantly lower than the 80 MPa weld. The hardness peak for the different forging pressures was justifiable through the microstructural observations. For the 110 MPa weld, a small amount of Al-Cu-Mg fine particles were dispersed at the vicinity of the interface (Figure 3a), so the peak hardness increased slightly compared to the base material. For 80 MPa weld, a larger number of fine particles were dispersed at the weld interface vicinity (Figure 3b), resulting in a higher peak hardness. For the 60 MPa weld, a cluster of copper fragments were entrained into the Al side (Figure 3c), resulting in a slight increase in the weld hardness. It is obvious, comparing Figure 3 to see the entrapment of particles and fragments at the weld interface in the 60 and 80 MPa welds.

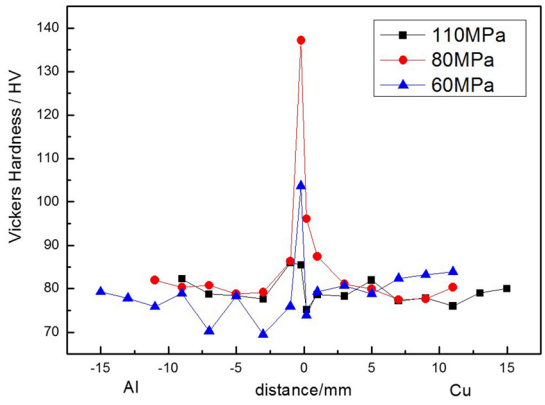

Figure 5. Vickers hardness distribution in the Al-Cu LFWs welded at different forging pressures.

3.3. Tensile strength and fracture behaviour

Tensile tests were performed for the welds at the three welding parameter conditions, with the results shown in Figure 6. In all the samples, fracture occurred in the elastic stage at the weld line, which suggested that the intermetallics played a significant role affecting the tensile strength, thus in this experiment, the yield strength and the elongation data of the samples could not be obtained. Furthermore, it was found that the tensile strength increases with the decrease in the forging pressure to 161 MPa at the lowest forging pressure investigated in this work.

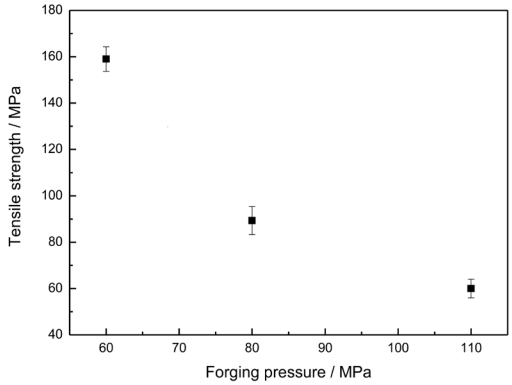

Figure 6. Tensile strength of the Al-Cu LFW joints at different forging pressures.

Figure 7 shows the fracture surface of the tensile test samples. A large number of dark grey areas (arrowed in Figure 7a) were visible in the fracture surface of the sample welded at the forging pressure of 110 MPa, which corresponded to the layered intermetallics observed in Figure 3a and 3d. At the forging pressure of 80 MPa, less layered phases were found in the fracture, but a large number of fine intermetallic particles were observed in the Al side (Figure 7b), corresponding to the Al-Cu-Mg particles in Figure 3b and 3e in the Al matrix, which resulted in a very high hardness. Hence, in this condition, the synergistic effect of the brittle intermetallic particles in the Al side and the layered intermetallics led to the fracture of the material. For the sample welded at 60 MPa, no layered intermetallics were observed, but a few particles could also be observed in the fracture surface, as shown in Figure 7c, corresponding to Figure 3c and 3f. In this condition, the tensile strength of the welded joint was the highest.

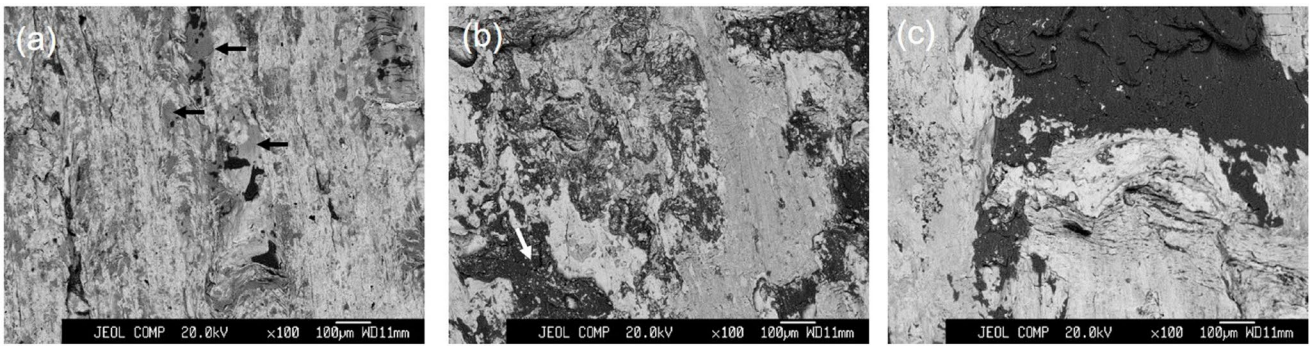

Figure 7. Backscattered electron micrographs of fracture surface of the welds observed from the copper part under different forging pressures: (a) 110 MPa; (b) 80 MPa; and (c) 60 MPa.

In Figure 6a, the gray zone shows the layered intermetallics (arrowed). In Figure 7b the arrows point at the intermetallic particles in the Al-rich region.

Figure 8 shows the EDX analyses of the Al-side of a fractured tensile sample of weld. Fractured occurred at the layered intermetallic phase indicated as “1” in the EDX analysis. The result showed that the Al, Cu, Mg ratio was 19.8:54.1:26.1 (in atomic%), which was close to Al_2CuMg.

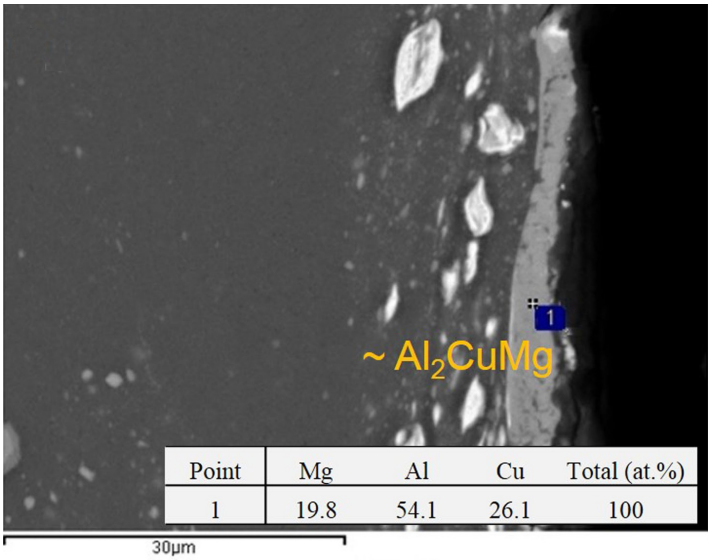

Figure 8. EDX analyses of the layered intermetallic phase of fractured tensile sample.

The mechanical properties of Al-Cu joints depend significantly on the Al-Cu interface, especially on the morphology of the intermetallic particles. Due to the inhomogeneous distribution, the intermetallic particles are likely to create a strain mismatch with the surrounding Al or Cu matrix, acting as a crack initiation point during mechanical testing. In this study, considering the Mg-content in AA5083 (4 wt. %), the presence of Mg affected the type of the intermetallic phase that formed.

In LFW, the process is a combination of thermal heating by friction and adiabatic heating due to the forging pressure. The forging pressure is one of the factors affecting the heat input during LFW, as suggested by Vairis et al. [15], and described by the following Equation 1:

$$LFW\ Heat\ input = \mu P_f \alpha 2\pi f \frac{1}{\sqrt{2}} \quad (1)$$

where, μ is the friction coefficient; P_f is the forging pressure; α is the oscillation amplitude; and f is the frequency of the oscillation.

The friction effect is reflected in the entrainment of Cu particles within the Al side. The entrainment of the Cu particles is due to the break up of the Cu asperities, which end up in the plasticised region in the weld. Depending on the forging pressure, the entrapped particles in the plasticised region might be forged out of the weld centre into the flash if a high forging pressure is used. Higher pressure also results in a higher heat input, which promotes the formation of the intermetallics by diffusion in the solid state, thus resulting in poorer mechanical properties. In lower pressures, the entrapped asperities do not get extruded out of the weld in the flash. Depending on the size of the entrapped Cu particles and the in-situ formed fine intermetallics, better strength might be achieved, compared with the high forging pressure.

4. Conclusions

This study investigated LFW of aluminium (AA5083) to copper (C101), to assess the impact of the forging pressure on the microstructure and mechanical properties, focusing on the in-situ generated intermetallic compounds due to the LFW procedure. The results showed that sound dissimilar LFW joints could be produced without obvious defect. The process led to the formation of intermetallic compounds across the weld interface, which affected the mechanical properties based on the morphology and extent of the intermetallic phases. In general, high forging pressure resulted in the formation of a layered Al_2CuMg phase, which was the most detrimental to the mechanical properties, compared with a scattered distribution of fragmented Cu-particles and intermetallics across the joint interface in lower to intermediate forging pressure.

Acknowledgements

The authors would like to acknowledge the financial support of the GDAS' Project of Science and Technology Development (grant numbers: 2017GDASCX-0117, 2018GDASCX-0117), Guangdong Science and Technology Department (grant number: 2017A050503004), and the Peal River S&T Nova Program of Guangzhou (grant number: 201806010126). Besides, NZ would like to acknowledge the Shaanxi Key Laboratory of Friction Welding Technologies for accessing the LFW facility as well as the technical support.

References

[1] Romero J, Attallah MM, Preuss M, Karadge M, Bray SE. Effect of the forging pressure on the microstructure and residual stress development in Ti-6Al-4V linear friction welds. Acta Materialia. 2009;57(18):5582-5592. http://dx.doi.org/10.1016/j.actamat.2009.07.055.

[2] Guo Y, Jung T, Chiu YL, Li H, Bray S, Bowen P. Microstructure and microhardness of Ti6246 linear friction weld. Materials Science and Engineering A. 2013;562:17-24. http://dx.doi.org/10.1016/j.msea.2012.10.089.

[3] Song X, Xie M, Hofmann F, Jun TS, Connolley T, Reinhard C, et al. Residual stresses in linear friction welding of aluminium alloys. Materials & Design. 2013;50:360-369. http://dx.doi.org/10.1016/j.matdes.2013.03.051.

[4] Li WY, Shi SX, Wang FF, Ma TJ, Li JL, Gao DL, et al. Heat reflux in flash and its effect on joint temperature history during linear friction welding of steel. International Journal of Thermal Sciences. 2013;67:192-199. http://dx.doi.org/10.1016/j.ijthermalsci.2012.12.004.

[5] Karadge M, Preuss M, Withers PJ, Bray S. Importance of crystal orientation in linear friction joining of single crystal to polycrystalline nickel-based superalloys. Materials Science and Engineering A. 2008;491(1-2):446-453. http://dx.doi.org/10.1016/j.msea.2008.04.064.

[6] Fratini L, Buffa G, Cammalleri M, Campanella D. On the linear friction welding process of aluminum alloys: experimental insights through process monitoring. CIRP Annals. 2013;62(1):295-298. http://dx.doi.org/10.1016/j.cirp.2013.03.056.

[7] Bhamji I, Moat RJ, Preuss M, Threadgill PL, Addison AC, Peel MJ. Linear friction welding of aluminium to copper. Science and Technology of Welding and Joining. 2012;17(4):314-320. http://dx.doi.org/10.1179/1362171812Y.0000000010.

[8] Dalgaard E, Wanjara P, Trigo G, Jahazi M, Comeau G, Jonas JJ. Linear friction welding of Al-Cu. Part 2: interfacial characteristics. Canadian Metallurgical Quarterly. 2011;50(4):360-370. http://dx.doi.org/10.1179/000844311X13112418194671.

[9] Xue P, Xiao BL, Ni DR, Ma ZY. Enhanced mechanical properties of friction stir welded dissimilar Al-Cu joint by intermetallic compounds. Materials Science and Engineering A. 2010;527(21-22):5723-5727. http://dx.doi.org/10.1016/j.msea.2010.05.061.

[10] Kah P, Vimalraj C, Martikainen J, Suoranta R. Factors influencing Al-Cu weld properties by intermetallic compound formation. International Journal of Mechanical and Materials Engineering. 2015;10(1):10. http://dx.doi.org/10.1186/s40712-015-0037-8.

[11] Bisadi H, Rasaee S, Fotoohi Y. Studying of tool rotation speed on mechanical properties of copper-Al5083 butt joint welded by friction stir welding. Proceedings of the Institution of Mechanical Engineers. Part B, Journal of Engineering Manufacture. 2014;229(10):1734-1741. http://dx.doi.org/10.1177/0954405414539491.

[12] Xia C, Li Y, Puchkov UA, Gerasimov SA, Wang J. Microstructure and phase constitution near the interface of Cu/Al vacuum brazing using Al-Si filler metal. Vacuum. 2008;82(8):799-804. http://dx.doi.org/10.1016/j.vacuum.2007.11.007.

[13] Lee SJ, Nakamura H, Kawahito Y, Katayama S. Effect of welding speed on microstructural and mechanical properties of laser lap weld joints in dissimilar Al and Cu sheets. Science and Technology of Welding and Joining. 2014;19(2):111-118. http://dx.doi.org/10.1179/1362171813Y.0000000168.

[14] Wanjara P, Dalgaard E, Trigo G, Mandache C, Comeau G, Jonas JJ. Linear friction welding of Al-Cu. Part 1: process evaluation. Canadian Metallurgical Quarterly. 2011;50(4):350-359. http://dx.doi.org/10.1179/000844311X13112418194644.

[15] Vairis A, Frost M. High frequency linear friction welding of a titanium alloy. Wear. 1998;217(1):117-131. http://dx.doi.org/10.1016/S0043-1648(98)00145-8.